

Piezoelectric Love Waves on Rotated Y -cut $mm2$ Substrates

Bernard Collet and Michel Destrade

Abstract—Consider a layer consisting of a $m3m$ dielectric crystal, with faces cut parallel to a symmetry plane. Then bond it onto a semi-infinite $mm2$ piezoelectric substrate. For a X - or Y -cut of the substrate, a Love wave can propagate in the resulting structure and the corresponding dispersion equation is derived analytically. It turns out that when the upper (free) face of the layer is metalized, a fully explicit treatment can also be conducted in the case of a Y -cut rotated about Z . In the case of a germanium layer over a potassium niobate substrate, the wave exists at any wavelength for X - and Y -cuts but this ceases to be the case for rotated cuts, with the appearance of forbidden ranges. By playing on the cut angle, the Love wave can be made to travel faster than, or slower than, or at the same speed as, the shear bulk wave of the layer. A by-product of the analysis is the derivation of the explicit secular equation for the Bleustein-Gulyaev wave in the substrate alone, which corresponds to an asymptotic behavior of the Love wave. The results are valid for other choices for the layer and for the substrate, provided they have the same, or more, symmetries.

I. INTRODUCTION

LAYERED structures, especially film/coating substrate systems, play an important role in microelectromechanical systems (MEMS) and in microelectronics packages. In order to achieve high performance, many surface acoustic wave (SAW) devices/sensors are designed as layered architectures such as, for instance, a dielectric, or piezoelectric, or a non-piezoelectric semiconductor (finite-thickness) layer deposited onto a (semi-infinite) piezoelectric substrate. For certain configurations, it is possible to have a one-component wave travel in the structure, in the direction of the interface; as this guided (shear-horizontal) Love wave leaves the upper face of the layer free of mechanical tractions, its amplitude varies sinusoidally through the thickness of the layer and then decays rapidly with depth in the substrate, and it is such that all fields are continuous at the layer/substrate interface.

Love waves in piezoelectric layered acoustic devices are most suitable for high-frequency filters because of their high phase velocity, and they also show great promise in biosensor applications with liquid environments because of their high sensitivity. Consequently, they have received much attention over the years. For example, Lardat *et al.* [1] found under which conditions a piezoelectrically

stiffened Love wave exists and they presented experimental and analytical results on surface wave delay lines. Kessenikh *et al.* [2] investigated surface Love waves in piezoelectric substrates of classes 6, 4, 6mm, 4mm, 622, and 422 with an isotropic dielectric layer. Hanhua and Xingjiao [3] studied Love waves for a structure formed by a 6mm piezoelectric layer and a 6mm piezoelectric substrate, with a common symmetry axis in the plane of the interface; Darinskii and Weihnacht [4] had a similar structure, of a $mm2$ piezoelectric layer and a $mm2$ piezoelectric substrate with common symmetry axes, one of which is aligned with the propagation direction and another is aligned with the normal to the interface. Jakoby and Vellekoop [5] reviewed the properties of Love waves and associated numerical methods for a piezoelectric/piezoelectric layered structure, when the substrate is a ST -cut quartz crystal; so did Ogilvy [6], with special emphasis on the mass-sensitivity loading of biosensors. The reader can find additional pointers to the literature on Love waves for piezoelectric sensors in those articles and in the references therein, as well as in the reviews by Farnell and Adler [7] or by Gulyaev [8].

The present work is concerned with the propagation of Love waves in a composite structure of a $m3m$ cubic dielectric (non-piezoelectric semiconductor) layer of finite thickness h , bonded onto a Y -cut rotated about Z , $mm2$ orthorhombic, piezoelectric substrate; see Fig. 1. The upper, mechanically free face of the layer is metalized and brought to zero electric potential (short-circuit). It turns out that, with this structure, the problem can be solved entirely by a direct analytic method which takes advantage of some “fundamental equations” derived elsewhere [9]–[11].

The dispersion relation can then be solved numerically for each mode and the solutions for the mechanical displacements, shear stresses, electric potentials, and electric inductions can be deduced explicitly. In passing, the explicit secular equations for the Bleustein-Gulyaev wave speed and for the limiting wave speed (substrate only, no overlayer) are found as a cubic and as a sextic in the squared wave speed, respectively, for rotated cuts. The special cases of a X -cut or Y -cut are treated separately. The effects of the angle of the cut on the phase velocity of the first modes are illustrated numerically for a specific layered structure, namely, a germanium layer over a potassium niobate substrate, and the appearance of a forbidden band of frequency is uncovered for a rotated cut, in sharp contrast with the non-rotated cuts where the waves exist for all frequencies.

Manuscript received March 2, 2006; accepted May 7, 2006.

The authors are with Laboratoire de Modélisation en mécanique, Université Pierre et Marie Curie, 75252 Paris Cedex, France (e-mail: destrade@lmm.jussieu.fr).

Digital Object Identifier 10.1109/TUFFC.2006.153

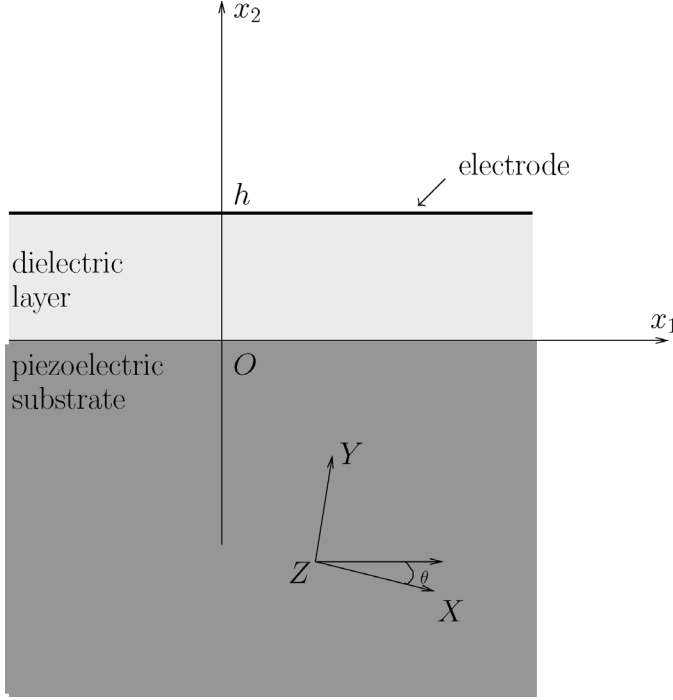


Fig. 1. Geometry of the layered structure.

II. THE LAYER

First, consider the upper layer, which consists of a cubic, m3m non-piezoelectric (semiconductor) crystal, with mass density $\hat{\rho}$. Let its symmetry axes be aligned with the axes x_1 , x_2 , and x_3 of a rectangular Cartesian coordinate system. For two-dimensional motions (independent of x_3), the out-of-plane equation of motion decouples from its in-plane counterpart and reads ($\leq x_2 \leq h$)

$$\hat{c}_{44} (\hat{u}_{3,11} + \hat{u}_{3,22}) = \hat{\rho} \hat{u}_{3,tt}, \quad (1)$$

where \hat{u}_3 is the out-of-plane mechanical displacement, \hat{c}_{44} is the transverse stiffness, and the comma denotes partial differentiation. For a solution in the form of an inhomogeneous wave traveling with speed v and wave number k in the x_1 direction, such as, say,

$$\hat{u}_3 = \hat{U}_3(kx_2) e^{ik(x_1-vt)}, \quad (2)$$

the equation of motion (1) reduces to

$$\hat{U}_3'' + \left(\frac{v^2}{\hat{v}^2} - 1 \right) \hat{U}_3 = 0, \quad \text{where } \hat{v} = \sqrt{\hat{c}_{44}/\hat{\rho}}, \quad (3)$$

and the prime denotes differentiation with respect to kx_2 . The general solution to this second-order differential equation is either Case (i):

$$\hat{U}_3(kx_2) = \hat{U}_3(0) \left(\cos \sqrt{\frac{v^2}{\hat{v}^2} - 1} kx_2 + A \sin \sqrt{\frac{v^2}{\hat{v}^2} - 1} kx_2 \right), \quad \text{when } v > \hat{v}, \quad (4)$$

or Case (ii):

$$\hat{U}_3(kx_2) = \hat{U}_3(0) \left(\cosh \sqrt{1 - \frac{v^2}{\hat{v}^2}} kx_2 + A \sinh \sqrt{1 - \frac{v^2}{\hat{v}^2}} kx_2 \right), \quad \text{when } v < \hat{v}, \quad (5)$$

where the constant A can be determined from the boundary condition at $x_2 = h$. This latter condition is that the upper face of the layer be free of mechanical tractions, so that $\hat{\sigma}_{23} = \hat{c}_{44} \hat{u}_{3,2}$ is zero there. Then it follows from (4) and (5) that $A = \tan \sqrt{v^2/\hat{v}^2 - 1} kh$ in Case (i), and that $A = -\tanh \sqrt{1 - v^2/\hat{v}^2} kh$ in Case (ii). Consequently, the mechanical field is now entirely known in the layer, up to the quantity $\hat{U}_3(0)$.

The procedure to find the electrical field is similar, and even simpler because the layer is not piezoelectric. Taking the electric potential $\hat{\phi}$ in the form, say,

$$\hat{\phi} = \hat{\varphi}(kx_2) e^{ik(x_1-vt)}, \quad (6)$$

Poisson's equation, $\Delta \hat{\phi} = 0$, reduces to

$$\hat{\varphi}'' = \hat{\varphi} = 0, \quad (7)$$

with general solution

$$\hat{\varphi}(kx_2) = \hat{\varphi}(0) (\cosh kx_2 + B \sinh kx_2), \quad (8)$$

where the constant B can be determined from the boundary condition on the upper face of the layer $x_2 = h$. A thin metallic film covers that face, and it is grounded to potential zero, $\hat{\varphi}(kh) = 0$. It then follows from (8) that $B = -\coth kh$ and, consequently, that the electrical field is now entirely known in the layer, up to the quantity $\hat{\varphi}(0)$.

For the problem at hand, only the values of the fields at the interface $x_2 = 0$ between the layer and the substrate are needed. Because the mechanical displacement \hat{u}_3 and the electrical potential $\hat{\phi}$ are in the forms (2) and (6), respectively, the mechanical traction $\hat{\sigma}_{23}$ and the electrical displacement \hat{D}_2 must also be of a similar form, due to the constitutive relations, $\hat{\sigma}_{23} = \hat{c}_{44} \hat{u}_{3,2}$ and $\hat{D}_2 = -\hat{\epsilon}_{11} \hat{\phi}_{,2}$, where $\hat{\epsilon}_{11}$ is the dielectric constant of the layer. Hence,

$$\hat{\sigma}_{23} = ik \hat{t}_{23}(kx_2) e^{ik(x_1-vt)}, \quad \hat{D}_2 = ik \hat{d}_2(kx_2) e^{ik(x_1-vt)}, \quad (9)$$

say. In particular, the conclusions drawn from the calculations conducted above are that at the layer/substrate interface,

$$\hat{t}_{23}(0) = -i \hat{c} \hat{U}_3(0), \quad \hat{d}_2(0) = -i \hat{\epsilon} \hat{\varphi}(0), \quad (10)$$

where

$$\begin{aligned} \hat{c} &= \hat{c}_{44} \sqrt{\frac{v^2}{\hat{v}^2} - 1} \tan \sqrt{\frac{v^2}{\hat{v}^2} - 1} kh, \quad \text{when } v > \hat{v}, \\ \hat{c} &= -\hat{c}_{44} \sqrt{1 - \frac{v^2}{\hat{v}^2}} \tanh \sqrt{1 - \frac{v^2}{\hat{v}^2}} kh, \quad \text{when } v < \hat{v}, \\ \hat{\epsilon} &= \hat{\epsilon}_{11} \coth kh. \end{aligned} \quad (11)$$

III. THE SUBSTRATE

The substrate occupies the half-space $x_2 \leq 0$ with the strong piezoelectric crystal, potassium niobate, KbNO_3 (orthorhombic $mm2$ symmetry). Cut the crystal along a plane containing the Z -axis and making an angle θ with the XZ plane. Let $x_1x_2x_3$ be the coordinate system obtained after the rotation

$$\begin{bmatrix} m & n & 0 \\ -n & m & 0 \\ 0 & 0 & 1 \end{bmatrix}, \quad \text{where } m = \cos \theta, \quad n = \sin \theta. \quad (12)$$

Yet again, for a two-dimensional motion (independent of x_3), the out-of-plane strain and stress decouple from their in-plane counterparts. Hence, with $u_1 = u_2 = 0$, $u_3 = u_3(x_1, x_2, t)$ for the mechanical displacement, and $\phi = \phi(x_1, x_2, t)$ for the electric potential, the constitutive relations yield $\sigma_{11} = \sigma_{22} = \sigma_{33} = \sigma_{12} = 0$ for the stress components and $D_3 = 0$ for the electrical displacement, and they reduce to

$$\begin{aligned} \sigma_{23} &= c_{44}u_{3,2} + c_{45}u_{3,1} + e_{14}\phi_{,1} + e_{24}\phi_{,2}, \\ \sigma_{31} &= c_{45}u_{3,2} + c_{55}u_{3,1} + e_{15}\phi_{,1} + e_{14}\phi_{,2}, \\ D_1 &= e_{14}u_{3,2} + e_{15}u_{3,1} - \epsilon_{11}\phi_{,1} - \epsilon_{12}\phi_{,2}, \\ D_2 &= e_{24}u_{3,2} + e_{14}u_{3,1} - \epsilon_{12}\phi_{,1} - \epsilon_{22}\phi_{,2}, \end{aligned} \quad (13)$$

where the c_{ij} , e_{ij} , and ϵ_{ij} are related to the corresponding quantities \tilde{c}_{ij} , \tilde{e}_{ij} , and $\tilde{\epsilon}_{ij}$ in the crystallographic coordinate system XYZ through tensor transformations [12] as

$$\begin{aligned} c_{44} &= m^2\tilde{c}_{44} + n^2\tilde{c}_{55}, & c_{55} &= n^2\tilde{c}_{44} + m^2\tilde{c}_{55}, \\ c_{45} &= mn(\tilde{c}_{44} - \tilde{c}_{55}), & e_{24} &= m^2\tilde{e}_{24} + n^2\tilde{e}_{15}, \\ e_{15} &= n^2\tilde{e}_{24} + m^2\tilde{e}_{15}, & e_{14} &= mn(\tilde{e}_{24} - \tilde{e}_{15}), \\ \epsilon_{11} &= m^2\tilde{\epsilon}_{11} + n^2\tilde{\epsilon}_{22}, & \epsilon_{22} &= n^2\tilde{\epsilon}_{11} + m^2\tilde{\epsilon}_{22}, \\ \epsilon_{12} &= mn(\tilde{\epsilon}_{22} - \tilde{\epsilon}_{11}). \end{aligned} \quad (14)$$

Now consider the x_2 -cut, x_1 -propagation of a shear-horizontal interface acoustic wave, that is, a motion with speed v and wave number k where the displacement field u_3 and the electric potential ϕ are of the form, say,

$$\{u_3, \phi\}(x_1, x_2, t) = \{U_3(kx_2), \varphi(kx_2)\}e^{ik(x_1 - vt)}, \quad (15)$$

with

$$U_3(-\infty) = 0, \quad \varphi(-\infty) = 0. \quad (16)$$

It follows from the constitutive relations (13) that the traction σ_{32} and the electric induction D_2 are of a similar form, say,

$$\{\sigma_{32}, D_2\}(x_1, x_2, t) = ik\{t_{32}(kx_2), d_2(kx_2)\}e^{ik(x_1 - vt)}, \quad (17)$$

where

$$t_{32}(-\infty) = 0, \quad d_2(-\infty) = 0. \quad (18)$$

The nontrivial part of the equations of piezoacoustics, $\sigma_{ij,j} = \rho u_{i,tt}$, $D_{i,i} = 0$ (where ρ is the mass density of the crystal), can be written as a second-order differential system [13]:

$$T \begin{bmatrix} U_3'' \\ \varphi'' \end{bmatrix} + 2iR \begin{bmatrix} U_3' \\ \varphi' \end{bmatrix} - [Q - (\rho v^2) J] \begin{bmatrix} U_3 \\ \varphi \end{bmatrix} = \begin{bmatrix} 0 \\ 0 \end{bmatrix}, \quad (19)$$

where

$$\begin{aligned} T &= \begin{bmatrix} c_{44} & e_{24} \\ e_{24} & -\epsilon_{22} \end{bmatrix}, & R &= \begin{bmatrix} c_{45} & e_{14} \\ e_{14} & -\epsilon_{12} \end{bmatrix}, \\ Q &= \begin{bmatrix} c_{55} & e_{15} \\ e_{15} & -\epsilon_{11} \end{bmatrix}, & J &= \begin{bmatrix} 1 & 0 \\ 0 & 0 \end{bmatrix}, \end{aligned} \quad (20)$$

or as a first-order differential system in the form

$$\xi' = iN\xi, \quad \text{where } \xi(kx_2) = [U_3, \varphi, t_{31}, d_2]^t; \quad (21)$$

N has the Stroh block structure

$$N = \begin{bmatrix} N_1 & N_2 \\ N_3 + (\rho v^2) J & N_1^t \end{bmatrix}, \quad (22)$$

with [14]

$$N_1 = -T^{-1}R, \quad N_2 = T^{-1}, \quad N_3 = RT^{-1}R - Q. \quad (23)$$

Here the components of N are easily computed from (20) and (23) by hand or using a computer algebra system.

Seeking a solution to (19) in the form $[U_3, \varphi]^t = [U_3(0), \varphi(0)]^t e^{ikqx_2}$, where q is constant, yields the propagation condition

$$\det [q^2T + 2qR + Q - (\rho v^2) J] = 0, \quad (24)$$

a quartic in q . Explicitly,

$$\begin{aligned} c_{44}^D q^4 + 2\frac{\epsilon_{12}}{\epsilon_{22}} c_{16}^D q^3 + (c_{45}^D - \rho v^2) q^2 \\ + 2\frac{\epsilon_{12}}{\epsilon_{22}} (c_{26}^D - \rho v^2) q + \frac{\epsilon_{11}}{\epsilon_{22}} (c_{55}^D - \rho v^2) = 0, \end{aligned} \quad (25)$$

where

$$\begin{aligned} c_{44}^D &= c_{44} + \frac{e_{24}^2}{\epsilon_{22}}, & c_{16}^D &= c_{44} + c_{45} \frac{\epsilon_{22}}{\epsilon_{12}} + 2\frac{e_{14}e_{24}}{\epsilon_{12}}, \\ c_{45}^D &= c_{55} + c_{44} \frac{\epsilon_{11}}{\epsilon_{22}} + 2\frac{e_{15}e_{24}}{\epsilon_{22}} + 4c_{45} \frac{\epsilon_{12}}{\epsilon_{22}} + 4\frac{e_{14}^2}{\epsilon_{22}}, \\ c_{55}^D &= c_{55} + \frac{e_{15}^2}{\epsilon_{11}}, & c_{26}^D &= c_{55} + c_{45} \frac{\epsilon_{11}}{\epsilon_{12}} + 2\frac{e_{15}e_{24}}{\epsilon_{12}}. \end{aligned} \quad (26)$$

Out of the four possible roots, only two have a negative imaginary part, insuring exponential decay as $x_2 \rightarrow -\infty$. Computing these qualifying roots analytically at $\theta = 0^\circ$ or 90° is straightforward, because then the quartic is a bi-quadratic. Otherwise, it is not an easy matter. Although it is actually possible to do so [15], [16], this paper follows

a different route and makes extensive use of the “fundamental equations” derived in [9]–[11]. They read

$$\boldsymbol{\xi}(0) \cdot M^{(n)} \bar{\boldsymbol{\xi}}(0) = 0, \quad \text{where } M^{(n)} = \begin{bmatrix} 0 & I \\ I & 0 \end{bmatrix} N^n, \quad (27)$$

and n is any positive or negative integer.

IV. THE LAYER/SUBSTRATE STRUCTURE

The continuity of all fields at the layer/substrate interface $x_2 = 0$ imposes the boundary conditions:

$$\begin{aligned} U_3(0) &= \hat{U}_3(0), & \varphi(0) &= \hat{\varphi}(0), \\ t_{23}(0) &= \hat{t}_{23}(0), & d_2(0) &= \hat{d}_2(0). \end{aligned} \quad (28)$$

Now the dispersion equations are derived explicitly. In the special cases of X - and Y -cuts, the dispersion equation is exact: if it is satisfied, then the Love wave exists. In other cases, the dispersion equation is rationalized: it has spurious roots, not corresponding to a true Love wave so that a subsequent validity check is necessary.

A. Special Cases $\theta = 0^\circ, 90^\circ$

For a X -cut or a Y -cut of the substrate, the analysis simplifies considerably; it leads to an exact dispersion equation and it does not require the use of the fundamental equations.

When $m = 1, n = 0$, or $m = 0, n = 1$, the parameters c_{45} , e_{14} , and ϵ_{12} vanish according to (14). Then in (20), $R \equiv 0$ also, and the quartic (24) becomes the following biquadratic [4]:

$$q^4 - Sq^2 + P = 0, \quad (29)$$

where the nondimensional quantities S and P are given by

$$\begin{aligned} -S &= \frac{c_{44}\epsilon_{11} + c_{55}\epsilon_{22} + 2e_{15}e_{24} - \epsilon_{22}(\rho v^2)}{c_{44}\epsilon_{22} + e_{24}^2}, \\ P &= \frac{c_{55}\epsilon_{11} + e_{15}^2 - \epsilon_{11}(\rho v^2)}{c_{44}\epsilon_{22} + e_{24}^2}. \end{aligned} \quad (30)$$

The relevant roots q_1 and q_2 come in one of the two following forms, either

$$q_1 = -i\beta_1, \quad q_2 = -i\beta_2, \quad (31a)$$

or

$$q_1 = -\alpha - i\beta, \quad q_2 = \alpha - i\beta, \quad (31b)$$

where $\beta_i > 0$ and $\beta > 0$. In either case, $q_1 + q_2$ has no real part and a negative imaginary part, and $q_1 q_2$ is a negative real number. Explicitly,

$$q_1 + q_2 = -i\sqrt{2\sqrt{P} - S}, \quad q_1 q_2 = -\sqrt{P}. \quad (32)$$

The associated eigenvectors $\boldsymbol{\zeta}^1$ and $\boldsymbol{\zeta}^2$ follow from (for instance) the third column of the adjoints to the matrices $N - q_1 I$ and $N - q_2 I$, as $\boldsymbol{\zeta}^i = [\mathbf{a}^i, \mathbf{b}^i]^t$, ($i = 1, 2$) where

$$\mathbf{a}^i = \left[q_i^2 + \frac{\epsilon_{11}}{\epsilon_{22}}, \frac{e_{24}}{\epsilon_{22}} q_i^2 + \frac{e_{15}}{\epsilon_{22}} \right]^t, \quad \mathbf{b}^i = q_i T \mathbf{a}^i, \quad (33)$$

(here T is given by (20), with components evaluated at 0° or 90°). Then the general solution to the equations of motion is of the form

$$\boldsymbol{\xi}(kx_2) = \gamma_1 e^{ikq_1 x_2} \boldsymbol{\zeta}^1 + \gamma_2 e^{ikq_2 x_2} \boldsymbol{\zeta}^2, \quad (34)$$

where γ_1 and γ_2 are constants.

At $x_2 = 0$, it can be split as

$$[U_3(0), \varphi(0)]^t = A\boldsymbol{\gamma}, \quad [t_{23}(0), d_2(0)]^t = B\boldsymbol{\gamma}, \quad (35)$$

where

$$A = [\mathbf{a}^1 | \mathbf{a}^2], \quad B = [\mathbf{b}^1 | \mathbf{b}^2], \quad \boldsymbol{\gamma} = [\gamma_1, \gamma_2]^t, \quad (36)$$

Now the boundary conditions (28) and (10) give the link

$$\begin{aligned} B\boldsymbol{\gamma} &= [\hat{t}_{23}(0), \hat{d}_2(0)]^t = \text{Diag}(-i\hat{c}, -i\hat{e}) [\hat{U}_3(0), \hat{\varphi}(0)]^t \\ &= -i \text{Diag}(\hat{c}, \hat{e}) A\boldsymbol{\gamma}, \end{aligned} \quad (37)$$

from which the dispersion equation follows as

$$|iBA^{-1} - \text{Diag}(\hat{c}, \hat{e})| = 0. \quad (38)$$

It is written in this form to take advantage of the many desirable properties of the surface impedance tensor iBA^{-1} [17]; thus, this matrix is Hermitian in the subsonic range (defined below), and of the compact form:

$$iBA^{-1} = \frac{i}{q_1 + q_2} \begin{bmatrix} \rho v^2 - c_{55} - c_{44}q_1q_2 & -e_{15} + e_{24}q_1q_2 \\ -e_{15} + e_{24}q_1q_2 & \epsilon_{11} - \epsilon_{22}q_1q_2 \end{bmatrix}. \quad (39)$$

Moreover, the eigenvalues of the aggregate impedance tensor in (38) are real monotonically decreasing functions of v for any fixed kh , so that the wave speed of each mode is obtained unambiguously from the roots of (38); see Shuvalov and Every [18].

Using the identities $q_1^2 + q_2^2 = S$ and $q_1^2 q_2^2 = P$ and the connections (30) and (32), the exact, explicit, dispersion equation is finally derived as

$$\left| \frac{\rho v^2 - c_{55} - c_{44}\sqrt{P}}{\sqrt{2\sqrt{P} - S}} + \hat{c} - \frac{e_{15} + e_{24}\sqrt{P}}{\sqrt{2\sqrt{P} - S}} \right| = 0, \quad (40)$$

which is a fully explicit equation, because \hat{c} and \hat{e} are defined in (10) and S and P in (30).

The dispersion equation is valid in the subsonic range, that is, as long as the speed is less than the limiting speed v_L , the smallest speed at which the biquadratic (29) ceases to have two roots q_1 and q_2 with a positive imaginary part. When q_1 and q_2 are of the form in (31a), then v_L is root to $P = 0$; when they are of the form in (31b), then v_L is root to $2\sqrt{P} = S$. In either case, the wave becomes homogeneous at $v = v_L$ because then the roots of the biquadratic are real; they are: $\pm q$, where $q = \sqrt{S_L}$ or $q = \sqrt{S_L/2}$, according to each case (here S_L is S given by (30) at $v = v_L$). The associated eigenvectors are $[\mathbf{a}, \pm \mathbf{b}]^t$, where

$$\mathbf{a} = \left[q^2 + \frac{\epsilon_{11}}{\epsilon_{22}}, \frac{e_{24}}{\epsilon_{22}} q^2 + \frac{e_{15}}{\epsilon_{22}} \right]^t, \quad \mathbf{b} = qT\mathbf{a}. \quad (41)$$

The vanishing of the wave away from the interface can no longer be ensured then, but the continuity of the fields at $x_2 = 0$ can. The conclusion is that the boundary conditions (28) and (10) lead to the following cut-off equation,

$$\begin{vmatrix} \left(c_{44} + \frac{e_{24}^2}{\epsilon_{22}} \right) q^2 + \frac{c_{44}\epsilon_{11} + e_{24}e_{15}}{\epsilon_{22}} & \hat{c} \left(q^2 + \frac{\epsilon_{11}}{\epsilon_{22}} \right) \\ e_{24} \frac{\epsilon_{11}}{\epsilon_{22}} - e_{15} & \hat{e} \left(\frac{e_{24}}{\epsilon_{22}} q^2 + \frac{e_{15}}{\epsilon_{22}} \right) \end{vmatrix} = 0. \quad (42)$$

This equation has an infinity of roots in kh (corresponding to the intersections of the graph of \tan with the graph of \coth). Each root $(kh)_L$, say, is a cut-off parameter for each dispersion mode, at which the Love wave ceases to exist.

Note that the dispersion relation (40) is consistent with the secular equation of a Bleustein-Gulyaev wave traveling in the substrate alone: as h tends toward zero, $\hat{c} \rightarrow 0$ and $\hat{e} \rightarrow \infty$, so that (40) reduces to $\rho v^2 - c_{55} = c_{44}\sqrt{P}$, which, once squared, coincides with the quadratic (56) obtained in the next Section. It is also consistent with the dispersion equation for a purely elastic Love wave. Indeed, by taking $e_{ij} \rightarrow 0$ and $\epsilon_{ij} \rightarrow 0$ in (30) and (40), the equation of Lardat *et al.* [1] is recovered:

$$\tan \sqrt{\frac{\hat{\rho}v^2 - \hat{c}_{44}}{\hat{c}_{44}}} kh = \frac{c_{44} \sqrt{\frac{c_{55} - \rho v^2}{c_{44}}}}{\hat{c}_{44} \sqrt{\frac{\hat{\rho}v^2 - \hat{c}_{44}}{\hat{c}_{44}}}}. \quad (43)$$

Finally, it is consistent with the dispersion equation of Love surface waves in an isotropic dielectric layer over a 6mm piezoelectric substrate [2], by the corresponding specialization.

B. Rotated Cut

Combining the boundary conditions (28) with the results for $\hat{t}_{23}(0)$ and $\hat{d}_2(0)$ of (10) gives the following form for $\boldsymbol{\xi}(0)$:

$$\boldsymbol{\xi}(0) = U_3(0) [1, \alpha, -i\hat{c}, -i\hat{e}\alpha]^t, \quad (44)$$

where $\alpha = \varphi(0)/U_3(0)$ is complex: $\alpha = \alpha_1 + i\alpha_2$, say. Then the fundamental relations (27) read

$$\begin{bmatrix} 1 \\ \bar{\alpha} \\ i\hat{c} \\ i\hat{e}\bar{\alpha} \end{bmatrix} \begin{bmatrix} M_{11}^{(n)} & M_{12}^{(n)} & M_{13}^{(n)} & M_{14}^{(n)} \\ M_{12}^{(n)} & M_{22}^{(n)} & M_{23}^{(n)} & M_{24}^{(n)} \\ M_{13}^{(n)} & M_{23}^{(n)} & M_{33}^{(n)} & M_{34}^{(n)} \\ M_{14}^{(n)} & M_{24}^{(n)} & M_{34}^{(n)} & M_{44}^{(n)} \end{bmatrix} \begin{bmatrix} 1 \\ \alpha \\ -i\hat{c} \\ -i\hat{e}\alpha \end{bmatrix} = 0, \quad (45)$$

or

$$\begin{aligned} & \left[M_{12}^{(n)} + \hat{c}\hat{e}M_{34}^{(n)} \right] (2\alpha_1) + \left[\hat{e}M_{14}^{(n)} - \hat{c}M_{23}^{(n)} \right] (2\alpha_2) \\ & + \left[M_{22}^{(n)} + \hat{e}^2M_{44}^{(n)} \right] (\alpha_1^2 + \alpha_2^2) = - \left[M_{11}^{(n)} + \hat{c}^2M_{33}^{(n)} \right]. \end{aligned} \quad (46)$$

Writing them for $n = -1, 1, 2$, and re-arranging the three resulting equations, leads to the following nonhomogeneous system of linear equations,

$$[\mathbf{k}_1 | \mathbf{k}_2 | \mathbf{k}_3] \mathbf{p} = -\mathbf{k}_4, \quad (47)$$

where $\mathbf{p} = [2\alpha_1, 2\alpha_2, \alpha_1^2 + \alpha_2^2]^t$ and $\mathbf{k}_1, \mathbf{k}_2, \mathbf{k}_3$, and \mathbf{k}_4 are the vectors with components:

$$\begin{aligned} & M_{12}^{(n)} + \hat{c}\hat{e}M_{34}^{(n)}, \quad \hat{e}M_{14}^{(n)} - \hat{c}M_{23}^{(n)}, \\ & M_{22}^{(n)} + \hat{e}^2M_{44}^{(n)}, \quad M_{11}^{(n)} + \hat{c}^2M_{33}^{(n)}, \end{aligned} \quad (48)$$

($n = -1, 1, 2$), respectively. Cramer's rule gives the unique solution to the system as

$$2\alpha_1 = -\Delta_1/\Delta, \quad 2\alpha_2 = -\Delta_2/\Delta, \quad \alpha_1^2 + \alpha_2^2 = -\Delta_3/\Delta, \quad (49)$$

where $\Delta = \det[\mathbf{k}_1 | \mathbf{k}_2 | \mathbf{k}_3]$, $\Delta_1 = \det[\mathbf{k}_4 | \mathbf{k}_2 | \mathbf{k}_3]$, $\Delta_2 = \det[\mathbf{k}_1 | \mathbf{k}_4 | \mathbf{k}_3]$, and $\Delta_3 = \det[\mathbf{k}_1 | \mathbf{k}_2 | \mathbf{k}_4]$. The dispersion equation follows then from the compatibility of the equalities (49):

$$\Delta_1^2 + \Delta_2^2 + 4\Delta_3\Delta = 0. \quad (50)$$

When (and if) this dispersion relation yields a real positive wave speed v for a given wave number k , it remains to be checked whether that speed corresponds to a valid solution. Proceed as follows. First recall that the exact boundary condition is of the form (38), where now the \mathbf{a}^i and \mathbf{b}^i ($i = 1, 2$) are defined by

$$\begin{aligned} \mathbf{a}^i &= \left[q_i^2 + 2\frac{\epsilon_{12}}{\epsilon_{22}} q_i + \frac{\epsilon_{11}}{\epsilon_{22}}, q_i^2 + 2\frac{e_{14}}{\epsilon_{22}} q_i + \frac{e_{15}}{\epsilon_{22}} \right]^t \\ \mathbf{b}^i &= (q_i T + R) \mathbf{a}^i. \end{aligned} \quad (51)$$

The computation of the corresponding surface impedance tensor iBA^{-1} is long but perfectly possible analytically; its components depend on q_1 and q_2 through the sum $q_1 + q_2$ and the product $q_1 q_2$. Now, having found a speed from (50), compute numerically the roots of the quartic (24). Select q_1 and q_2 , the roots with negative imaginary parts (if there are no such roots, then v is not valid.) Then compute

$q_1 + q_2$, $q_1 q_2$, and iBA^{-1} , and check whether the exact boundary condition (38) is satisfied.

Finally, it is also possible to determine exactly the limiting speed v_L above which the decay condition is no longer insured. Fu [15] shows that v_L is the smallest root of $D = 0$, where D is the discriminant of the cubic resolvent associated with the quartic (24). Thus, rewrite the quartic (24) in its canonical form, say,

$$p^4 + rp^2 + sp + t = 0, \quad (52)$$

using the substitution $q = p - (1/2)(\epsilon_{12}/\epsilon_{22})(c_{16}^D/c_{44}^D)$. Then,

$$D = -4(12t + r^2)^3 + (-72tr + 2r^3 + 27s^2)^2. \quad (53)$$

Using a computer algebra system, it was found that the equation $D = 0$ is a sextic in the squared wave speed.

V. BLEUSTEIN-GULYAEV WAVE AS $h \rightarrow 0$

Shuvalov and Every [18] show that a great variety of asymptotic behaviors arises for an interface wave on a coated half-space. When the thickness of the layer vanishes here, the asymptotic behavior of the Love wave in the layer/substrate structure is that of a shear-horizontal surface wave propagation over the piezoelectric substrate alone (the Bleustein-Gulyaev wave [19], [20]). For such a wave, with metalized boundary conditions, the vector $\xi(0)$ takes the form

$$\xi(0) = [U_3(0), 0, 0, d_3(0)]^t = U_3(0) [1, 0, 0, \alpha]^t, \quad (54)$$

where $\alpha = d_3(0)/U_3(0)$ is complex. The fundamental relations (27), written for, say, $n = -1, 1, 2$, can be arranged as

$$\begin{bmatrix} M_{11}^{(-1)} & M_{14}^{(-1)} & M_{44}^{(-1)} \\ M_{11}^{(1)} & M_{14}^{(1)} & M_{44}^{(1)} \\ M_{11}^{(2)} & M_{14}^{(2)} & M_{44}^{(2)} \end{bmatrix} \begin{bmatrix} 1 \\ \alpha + \bar{\alpha} \\ \alpha \bar{\alpha} \end{bmatrix} = \begin{bmatrix} 0 \\ 0 \\ 0 \end{bmatrix}, \quad (55)$$

a homogeneous linear system of three equations. Its solution is nontrivial when the determinant of the 3×3 matrix on the left-hand side is zero. The resulting secular equation is a cubic in ρv^2 . At $\theta = 0^\circ$ and $\theta = 90^\circ$, the secular equation factorizes into the product of a term linear in ρv^2 and a term quadratic in ρv^2 . In particular, at $\theta = 0$ the quadratic is

$$(\rho v^2 - \tilde{c}_{55})^2 + \tilde{c}_{44}^2 \frac{(\rho v^2 - \tilde{c}_{55}) \tilde{\epsilon}_{11} - \tilde{e}_{15}^2}{\tilde{c}_{44} \tilde{\epsilon}_{22} + \tilde{e}_{24}^2} = 0. \quad (56)$$

Further, $\tilde{c}_{44} = \tilde{c}_{55}$, $\tilde{\epsilon}_{11} = \tilde{\epsilon}_{22}$, and $\tilde{e}_{24} = \tilde{e}_{15}$ for the 6mm symmetry, and (56) then simplifies into the product of ρv^2 and the linear equation in ρv^2 of Bleustein and Gulyaev.

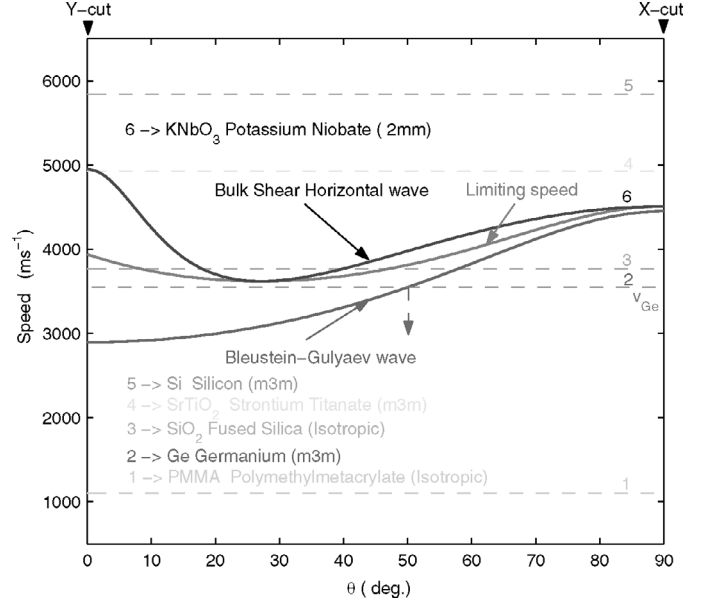


Fig. 2. Solid curves: Variations of the Bleustein-Gulyaev wave and limiting wave speeds with cut angle in a homogeneous KbNO_3 substrate. Horizontal dashed lines: Speed of a (bulk) shear wave in PMMA (1), Ge (2), SiO_2 (3), SrTiO_2 , and Si (5).

Now for KbNO_3 , the material parameters of interest are [21]: $\tilde{c}_{44} = 7.43$, $\tilde{c}_{55} = 2.5 (10^{10} \text{ N/m}^2)$, $\tilde{e}_{24} = 11.7$, $\tilde{e}_{15} = 5.16 (\text{C/m}^2)$, $\tilde{\epsilon}_{11} = 34\epsilon_0$, $\tilde{\epsilon}_{22} = 780\epsilon_0$ ($\epsilon_0 = 8.854 \times 10^{-12} \text{ F/m}$), and $\rho = 4630 \text{ kg/m}^3$. Using these values, the corresponding parameters in the rotated coordinate system follow from (14), and, in turn, T , R , and Q follow from (20), N from (22)–(23), and $M^{(n)}$ from (27). Then the cubic secular equation is solved for v for any value of the cut angle θ . Out of the three possible roots, only one may correspond to the Bleustein-Gulyaev wave ([22] explains how the adequate root is selected.) It turns out that the wave exists for all angles, with a speed v_{BG} (say) increasing from 2895.35 m/s at $\theta = 0^\circ$ to 4450.85 m/s at $\theta = 90^\circ$. Fig. 2 shows the dependence in θ , and is in agreement with the plots obtained by Nakamura and Oshiki [23] and by Mozhaev and Weihnacht [24].

Fig. 2 also displays the speed of the bulk shear wave in a germanium layer, for which [25] $\hat{c}_{44} = 67.1 \times 10^{10} \text{ N/m}^2$, $\hat{\epsilon}_{11} = 16.6\epsilon_0$, and $\hat{\rho} = 5330 \text{ kg/m}^3$; here, $\hat{v} = 3550.31 \text{ m/s}$. The angle at which $v_{BG} = \hat{v}$ is $\theta_0 = 50.0817^\circ$. The variation of the limiting speed v_L in KbNO_3 with the angle of cut is shown as well, and that plot is also in agreement with the plot of Mozhaev and Weihnacht [24].

VI. DISPERSION CURVES

A. Special Case $\theta = 0^\circ$

At $\theta = 0^\circ$ and $kh = 0$, the interface wave travels in the substrate alone, with the Bleustein-Gulyaev wave speed of 2895.35 m/s. The limiting speed (found here as the root of $2\sqrt{P} = S$) is $v_L = 3939.33 \text{ m/s}$. The speed of the fundamental mode starts at the Bleustein-Gulyaev wave

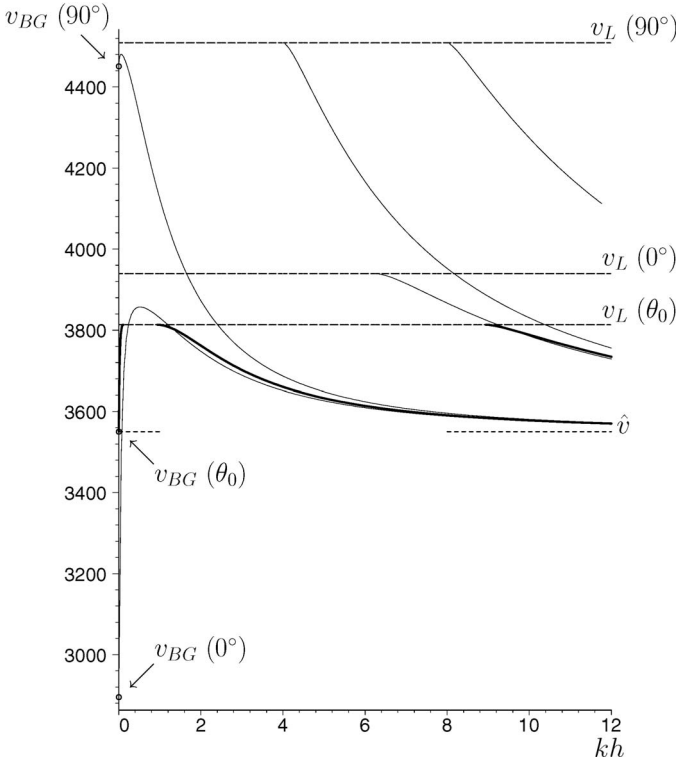


Fig. 3. Dispersion curves at $\theta = 0^\circ$, θ_0 , and 90° .

speed at $kh = 0$, increases to a maximum speed of about 3857.18 m/s at $kh = 0.517$, and then decreases toward the shear bulk speed of the layer, $\hat{v} = 3550.31$ m/s. In the narrow range where kh is smaller than 7.08436×10^{-2} , the speed v of the fundamental mode wave is smaller than \hat{v} . The fundamental mode exists for all values of kh .

The speeds of the subsequent modes start from the limiting speed v_L at $(kh)_L$ and tend toward \hat{v} in a monotonically decreasing manner. The cut-off parameter $(kh)_L$ for the first mode, second mode, and third mode is: 6.24, 12.75, and 19.27, respectively. Fig. 3 shows the dispersion curves for the fundamental mode and for the first mode. Qualitatively, the plots echo those of Kielczynski *et al.* [26] who considered a 6mm substrate covered with a “depolarized” layer.

B. Special Case $\theta = 90^\circ$

At $\theta = 90^\circ$ and $kh = 0$, the limiting speed is the root of $P = 0$; here, $v_L = 4508.73$ m/s. The speed of the fundamental mode starts at the Bleustein-Gulyaev wave speed of 4450.85 m/s at $kh = 0$, increases to a maximum speed of about 4480.69 m/s at $kh = 0.0581$, and then decreases toward the shear bulk speed of the layer, $\hat{v} = 3550.31$ m/s. Here, too, the fundamental mode exists for all values of kh .

The speeds of the subsequent modes start from the limiting speed v_L at $(kh)_L$ and decrease toward \hat{v} . The cut-off parameter $(kh)_L$ for the first mode, second mode, and third mode is 4.05, 8.06, and 12.06, respectively. Fig. 3 shows the dispersion curves for the fundamental mode and for the first and second modes.

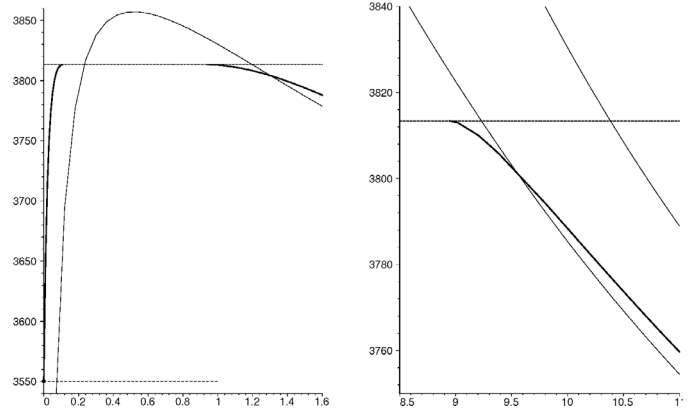


Fig. 4. Zooms for the dispersion of (a) the fundamental mode and (b) the first mode at $\theta = \theta_0$ (thick curves) and at $\theta = 0^\circ$, 90° (thin curves).

C. Special Case $\theta = \theta_0$

As an example of a rotated cut, consider the case where the speed of the Bleustein-Gulyaev wave in the substrate is equal to the shear wave speed in the layer; this occurs at $\theta = \theta_0 = 50.08^\circ$; see the vertical arrow in Fig. 2. For this cut, the limiting speed is $v_L = 3813.36$ m/s. Starting from $v_{BG} = \hat{v}$ at $kh = 0$, the speed of the fundamental mode increases rapidly with kh . At $kh = 0.1131$, $v = v_L$ and the wave ceases to exist. This state of affairs continues until kh reaches 0.9410, after which the wave exists and its speed decreases toward \hat{v} . Hence, a forbidden band of frequencies emerges for the fundamental mode, in clear contrast with the situation for non-rotated cuts. Note that the dispersion relation (50) actually gives roots below v_L in that range, which must nevertheless be discarded as they do not satisfy the exact boundary condition (38).

Here the first higher-order mode starts at the cut-off parameter $(kh)_L$ of 8.946 with v_L and then decreases toward \hat{v} . Fig. 4 provides a zoom into the dispersion curves of the fundamental mode around the forbidden band and of the first mode up to $kh = 11$.

In this example, the layered structure supports a shear-horizontal wave which in the long and short wavelength ranges travels with the speed of the layer’s bulk shear wave; in the intermediate range, the wave either does not exist, or travels at a greater speed.

VII. CONCLUDING REMARKS

The analysis conducted in the paper showed that the problem of a piezoelectric Love wave in a dielectric m3m layer over a rotated Y-cut mm2 substrate could be solved explicitly by the derivation of a rationalized dispersion equation.

Of course, it must be noted that the boundary conditions were special; here the upper surface of the structure is metalized and grounded. It is likely that more general boundary conditions (e.g., free surface) would lead to an intractable, or at least impractical, analytic treatment.

On the other hand, a certain degree of generality was achieved. Hence the substrate can be taken as any rotated Y -cut crystal with mm2 or 4mm symmetries (or, of course, with 6mm symmetry). Here the numerical results used the constants of potassium niobate because of its strong electromechanical coupling [23], [24]. Also, the parameters of any dielectric material with m3m symmetry can be used in the formulas derived in the paper. Here, germanium was selected because its bulk shear wave speed is always below the limiting speed for any angle of cut (a “slow” layer; see the horizontal dashed line 2 on Fig. 2); similarly a layer of polymethylmetacrylate (PMMA, isotropic) could have been selected; see the horizontal dashed line 1 on Fig. 2. In contrast, a layer of silicon (m3m) is always “faster” than the substrate; see the horizontal dashed line 5 on Fig. 2. Thus there is only a single, truncated, corresponding dispersion curve: that of the fundamental mode, increasing rapidly from the speed of the Bleustein-Gulyaev speed to the limiting speed as the dispersion parameter kh increases. Intermediate behaviors are depicted, for instance, by fused silica (isotropic, horizontal dashed line 3) or strontium titanate (m3m, horizontal dashed line 4).

Complementary results, including depth profiles, are presented in a companion paper [27].

REFERENCES

- [1] C. Lardat, C. Maerfeld, and P. Tournois, “Theory and performance of acoustical dispersive surface wave delay lines,” *Proc. IEEE*, vol. 59, pp. 355–368, 1971.
- [2] G. G. Kessenikh, V. N. Lyubimov, and L. A. Shuvalov, “Love surface waves in piezoelectrics,” *Sov. Phys. Crystallogr.*, vol. 27, pp. 267–270, 1982.
- [3] F. Hanhua and L. Xingjiao, “Shear-horizontal surface waves in a layered structure of piezoelectric ceramics,” *IEEE Trans. Ultrason., Ferroelect., Freq. Contr.*, vol. 40, pp. 167–170, 1993.
- [4] A. N. Darinskii and M. Weihnacht, “Supersonic Love waves in strong piezoelectrics of symmetry mm2,” *J. Appl. Phys.*, vol. 90, pp. 383–388, 2001.
- [5] B. Jakoby and M. J. Vellekoop, “Properties of Love waves: Applications in sensors,” *Smart Mater. Struct.*, vol. 6, pp. 668–679, 1997.
- [6] J. A. Ogilvy, “The mass-loading sensitivity of acoustic Love waves biosensors in air,” *J. Phys. D: Appl. Phys.*, vol. 30, pp. 2497–2501, 1997.
- [7] G. W. Farnell and E. L. Adler, “Elastic wave propagation in thin layers,” in *Physical Acoustics*, vol. 9, W. P. Mason and R. N. Thurston, Eds. New York: Academic, 1972, pp. 35–127.
- [8] Y. V. Gulyaev, “Review of shear surface acoustic waves in solids,” *IEEE Trans. Ultrason., Ferroelect., Freq. Contr.*, vol. 45, pp. 935–938, 1998.
- [9] M. Destrade, “Elastic interface acoustic waves in twinned crystals,” *Int. J. Solids Struct.*, vol. 40, pp. 7375–7383, 2003.
- [10] M. Destrade, “Explicit secular equation for Scholte waves over a monoclinic crystal,” *J. Sound Vib.*, vol. 273, pp. 409–414, 2004.
- [11] M. Destrade, “On interface waves in misoriented pre-stressed incompressible elastic solids,” *IMA J. Appl. Math.*, vol. 70, pp. 3–14, 2005.
- [12] B. A. Auld, *Acoustic Fields and Waves in Solids*. Malabar, FL: Krieger, 1990, p. 275.
- [13] V. G. Mozhaev and M. Weihnacht, “Sectors of nonexistence of surface acoustic waves in potassium niobate,” in *Proc. IEEE Ultrason. Symp.*, vol. 1, 2002, pp. 391–395.
- [14] T. C. T. Ting, *Anisotropic Elasticity: Theory and Applications*. New York: Oxford Univ. Press, 1996.
- [15] Y. B. Fu, “An explicit expression for the surface-impedance matrix of a generally anisotropic incompressible elastic material in a state of plane strain,” *Int. J. Non-linear Mech.*, vol. 40, pp. 229–239, 2005.
- [16] M. Destrade and Y. B. Fu, “The speed of interface waves polarized in a symmetry plane,” *Int. J. Eng. Sci.*, vol. 44, pp. 26–36, 2006.
- [17] M. Abbudi and D. M. Barnett, “On the existence of interfacial (Stoneley) waves in bonded piezoelectric half-spaces,” *Proc. Roy. Soc. London A*, vol. 429, pp. 587–611, 1990.
- [18] A. L. Shuvalov and A. G. Every, “Some properties of surface acoustic waves in anisotropic-coated solids, studied by the impedance method,” *Wave Motion*, vol. 36, pp. 257–273, 2002.
- [19] J. L. Bleustein, “A new surface wave in piezoelectric materials,” *Appl. Phys. Lett.*, vol. 13, pp. 412–413, 1968.
- [20] Y. V. Gulyaev, “Electroacoustic surface waves in piezoelectric materials,” *J. Expl. Theoret. Phys. Lett.*, vol. 9, pp. 37–38, 1969.
- [21] M. Zgonik, R. Schlessler, I. Biaggio, E. Voit, J. Tscherry, and P. Günter, “Material constants of KNbO₃ relevant for electro-and acousto-optics,” *J. Appl. Phys.*, vol. 74, p. 1287, 1993.
- [22] B. Collet and M. Destrade, “Explicit secular equations for piezoacoustic surface waves: Shear-horizontal modes,” *J. Acoust. Soc. Amer.*, vol. 116, pp. 3432–3442, 2004.
- [23] K. Nakamura and M. Oshiki, “Theoretical analysis of horizontal shear mode piezoelectric surface acoustic waves in potassium niobate,” *Appl. Phys. Lett.*, vol. 71, pp. 3203–3205, 1997.
- [24] V. G. Mozhaev and M. Weihnacht, “Incredible negative values of effective electromechanical coupling coefficient for surface acoustic waves in piezoelectrics,” *Ultrasonics*, vol. 37, pp. 687–691, 2000.
- [25] W. Martienssen and H. Warlimont, Eds. *Springer Handbook of Condensed Matter and Materials Data*. Berlin: Springer, 2005.
- [26] P. J. Kielczynski, W. Pajewski, and M. Szalewski, “Shear-horizontal surface waves on piezoelectric ceramics with depolarized surface layer,” *IEEE Trans. Ultrason., Ferroelect., Freq. Contr.*, vol. 36, pp. 287–293, 1989.
- [27] B. Collet and M. Destrade, “Onde de Love piézoacoustique,” in *Proc. 8^{ème} Cong. Français Acoust.*, 2006, p. 4. (in French)



Bernard Collet holds a B.Sc., an M.Sc., a Ph.D., and a Thèse d’Etat in Mathematics - Mechanics from the Faculté des Sciences de Paris, France.

He made his academic career at the Université Pierre et Marie Curie, Paris, France, and is currently Professor of Mechanics, based at the Laboratoire de Modélisation en Mécanique. He is also in charge of the Undergraduate and Postgraduate Degrees in Mechanical Engineering at the Ecole Polytechnique Universitaire and of the Undergraduate



Michel Destrade was born in Bordeaux, France, in 1968. He holds a B.Sc. and an Agrégation in Physics from the Ecole Normale Supérieure, Cachan, France, and an M.Sc. and a Ph.D. in Mathematical Physics from University College, Dublin, Ireland.

He worked as an Instructor to native High School students in Nouméa, New Caledonia; as a High School Physics teacher in Rennes, France; and as a Visiting Assistant Professor in Mathematics at Texas A&M University, College Station, TX. He is now a Chargé de

Recherche with the French Centre National de la Recherche Scientifique (CNRS), and is based at the Laboratoire de Modélisation en Mécanique, Université Pierre et Marie Curie, Paris, France.